

Pressure-enhanced f -electron orbital weighting in UTe_2 mapped by quantum interferometry

T. I. Weinberger,¹ Z. Wu,¹ A. J. Hickey,¹ D. E. Graf,² G. Li,^{3,4} P. Wang,^{3,4} R. Zhou,^{3,4} A. Cabala,⁵ J. Pu,⁶ V. Sechovský,⁵ M. Vališka,⁵ G. G. Lonzarich,¹ F. M. Grosche,¹ and A. G. Eaton^{1,*}

¹*Cavendish Laboratory, University of Cambridge,*

JJ Thomson Avenue, Cambridge, CB3 0HE, United Kingdom

²*National High Magnetic Field Laboratory, Tallahassee, Florida, 32310, USA*

³*Beijing National Laboratory for Condensed Matter Physics,*

Institute of Physics, Chinese Academy of Sciences, Beijing 100190, China

⁴*School of Physical Sciences, University of Chinese Academy of Sciences, Beijing 100190, China*

⁵*Charles University, Faculty of Mathematics and Physics,*

Department of Condensed Matter Physics, Ke Karlovu 5, Prague 2, 121 16, Czech Republic

⁶*School of Physics and Astronomy, Shanghai Jiao Tong University, Shanghai, 200240, China*

(Dated: March 7, 2024)

The phase landscape of UTe_2 features a remarkable diversity of superconducting phases under applied pressure and magnetic field. Recent quantum oscillation studies at ambient pressure have revealed the quasi-2D Fermi surface of this material. However, the pressure-dependence of the Fermi surface remains an open question. Here we track the evolution of the UTe_2 Fermi surface as a function of pressure up to 19.5 kbar by measuring quantum interference oscillations. We find that in sufficient magnetic field to suppress both superconductivity at low pressures and incommensurate antiferromagnetism at higher pressures, the quasi-2D Fermi surface found at ambient pressure smoothly connects to that at 19.5 kbar, with no signs of a reconstruction over this pressure interval. The warping of the cylindrical Fermi sheets continuously increases with pressure, which is consistent with increased f -orbital contribution at the Fermi level, up to and beyond the critical pressure at which superconductivity is truncated. These findings highlight the value of high pressure quantum interference measurements as a new probe of the electronic structure in heavy fermion materials.

Quantum oscillation (QO) measurements are a powerful direct probe of a material's Fermi surface (FS) [1]. The Shubnikov-de Haas (SdH) [2] and de Haas-van Alphen (dHvA) [3] effects measure QOs respectively in the electrical transport and magnetization of metals. These techniques are premised on Landau quantization of itinerant quasiparticles' energy levels in a magnetic field, leading to oscillatory components in derivatives of the free energy (or the density of states) that relate directly to the Fermi surface geometry and carrier effective masses [4]. In sufficiently high magnetic fields magnetic breakdown can occur, whereby quasiparticles tunnel between FS sheets, the detection of which yields information about the spacing of FS sheets in relation to each other [5–7].

Analogous to the dHvA and SdH effects, in materials with sufficiently close FS sheets for magnetic breakdown to occur in experimentally accessible magnetic field strengths, quantum interference oscillations (QIOs) can be observed in transport measurements at high field [8, 9]. These stem from interference between quasiparticle orbits that branch into separate paths along the FS before later recombining, typically with one quasiparticle having tunnelled across to another FS sheet and then back again. QIOs thus yield valuable information about how FS sheets connect and span the Brillouin zone. QIOs

have been observed in a variety of metals, including elemental magnesium [9], quasi-2D organic superconductors [10, 11] and recently in the heavy fermion superconductor UTe_2 [12, 13].

In the context of heavy fermion systems, QIO measurements are especially powerful, because compared to dHvA or SdH oscillations they can persist to higher temperatures. This is because the observed frequencies and amplitudes are determined by the *differences* between quasiparticle orbit areas and their effective masses and thus can be observed to much higher temperatures than oscillations stemming directly from Landau quantization [1].

The heavy fermion dichalcogenide UTe_2 crystallizes in a body-centred orthorhombic structure ($Immm$ symmetry, space group 71) [14]. At ambient pressure and magnetic field it possesses an unconventional superconducting state below a critical temperature $T_c = 2.1$ K, which exhibits numerous characteristics of odd-parity pairing [15–17]. Under the application of either pressure or magnetic field (or both) several other distinct superconducting phases are accessed [16, 18–24], including one which persists to spectacularly high fields in excess of 60 T [25]. At a critical pressure of ≈ 15 kbar superconductivity is abruptly quenched, and an incommensurate antiferromagnetically (AFM) ordered state has been observed at low temperatures [26].

The normal state electronic properties of UTe_2 at ambient pressure have been probed by angle-resolved pho-

* alex.eaton@phy.cam.ac.uk

toemission spectroscopy (ARPES) and dHvA effect measurements [27–29], which have revealed a remarkably simple FS consisting of two undulating cylindrical sheets, one hole-type and the other electron-type. Slow oscillations observed in contactless resistivity measurements by the tunnel diode oscillator (TDO) method in high magnetic fields were reported to be characteristic of an additional, small, 3D FS pocket [12] – but no signature of this pocket was seen in either dHvA [28, 29] nor SdH [29] effect measurements. However, subsequent high-field measurements reproduced the observation of ref. [12], but found that the slow oscillations are rapidly suppressed within a 20° rotation away from the crystallographic a -axis [13], inconsistent with a 3D Fermi pocket scenario. Instead, these oscillations can be attributed to QIOs due to their very light (apparent) effective masses – inconsistent with an f -electron pocket but very consistent with the close spacing in k -space and pronounced undulations of the FS sheets previously revealed by dHvA measurements [29].

Understanding how the FS of UTe_2 evolves under the application of hydrostatic pressure is key to unpicking the rich interplay between the magnetic fluctuations, the formation of superconductivity and the underlying heavy fermion physics of this intriguing material [16]. Here, we report a high magnetic field study of the pressure dependence of quantum interference oscillations in UTe_2 for magnetic field $\mu_0 H \parallel a$. We argue that these QIOs arise from paths that wrap around the k -space area enclosed between the cylindrical Fermi sheets (normal to k_x) [13]. We find that this area continuously increases from 0 to 20 kbar for $\mu_0 H > 15$ T. This means that, for sufficient H to access the paramagnetic normal state above the AFM phase, the UTe_2 FS is smoothly connected over this entire pressure interval. Furthermore, we show that this growth in enclosed area relates to increased warping along the axis of the cylindrical sheets, which is characteristic of increased f -orbital contribution at the Fermi level as pressure is increased.

Methods – single crystal UTe_2 specimens were grown by the molten salt flux (MSF) technique [17] by the procedure given in ref. [29]. Samples were oriented by Laue diffractometry and mounted inside cylindrical coils (with the axis of the coil $\parallel a$) before loading into pressure cells. Daphne 7575 oil was used as the pressure medium [30], with each pressure point calibrated by ruby fluorescence [31]. Contactless resistivity measurements were made by the TDO technique [32] similar to the methodology in e.g. ref. [33]. Experiments were conducted in a resistive magnet up to 41.5 T fitted with a ^3He cryostat at the National High Magnetic Field Lab, Florida, USA; and in a superconducting magnet up to 30 T with a dilution refrigerator at the Synergetic Extreme Condition User Facility, Chinese Academy of Sciences, Beijing, China.

Results – Figure 1 shows QIOs in the contactless resistivity of UTe_2 . These QIOs correspond to the area between the cylindrical Fermi sheets, normal to k_x , which is shaded in red in panel (b). Panel (c) shows the evolu-

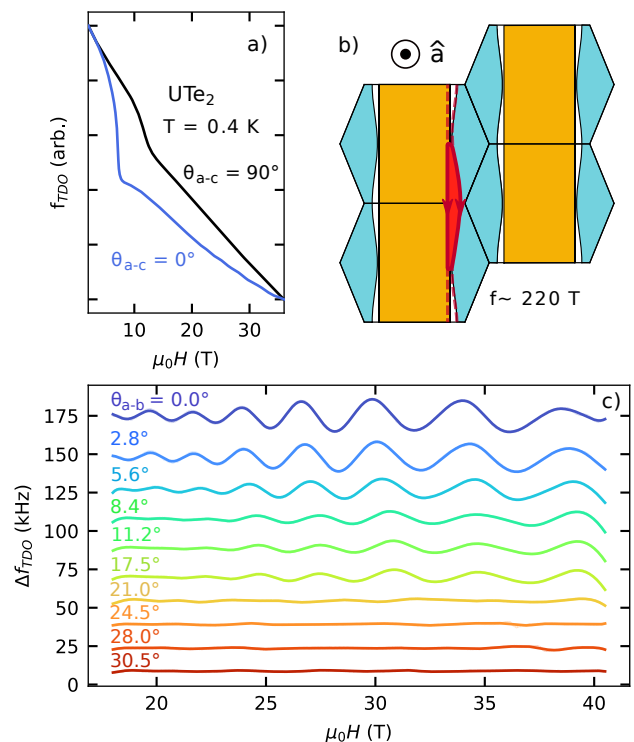


FIG. 1. (a) Contactless resistivity of UTe_2 measured by the change in frequency of a TDO circuit, f_{TDO} , for magnetic field orientations $H \parallel a$ ($\theta_{a-c} = 0^\circ$) and $H \parallel c$ ($\theta_{a-c} = 90^\circ$). (b) Side-view of the UTe_2 FS cylinders (adapted from ref. [29]). The $[100]$ direction (crystallographic a -axis) is oriented into the page. The red shaded area corresponds to the enclosed k -space area, between the FS cylinders, which yields a QIO frequency of ≈ 210 T. (c) QIOs for rotations of the magnetic field orientation from $H \parallel a$ towards $H \parallel b$. After 21.0° of rotation from $H \parallel a$ the QIO amplitude is drastically suppressed.

tion of the oscillatory waveform for successive magnetic field tilt angles in the $b - a$ plane, starting at $H \parallel a$ (i.e. $\theta_{a-b} = 0.0^\circ$). Six periods are clearly resolved over the field interval of 20–41 T for $\theta_{a-b} \leq 17.5^\circ$. However, the amplitude of the QIOs diminishes sharply with rotation away from the a -axis, and for $\theta_{a-b} \geq 21.0^\circ$ we no longer resolve any oscillations. This is consistent with our previous study of QIOs rotating in the $a - c$ plane, where the QIOs were found to be sharply suppressed for $\theta_{a-c} \geq 20^\circ$ [13]. Within the QIO interpretation outlined above, interfering paths enclosing the red shaded area of Fig. 1b only exist for fields close to the a -axis, causing the observed rapid suppression of QIO at higher inclinations [1, 10].

Figure 2 shows QIOs in the contactless resistivity of UTe_2 for the fixed magnetic field orientation $H \parallel a$ at selected pressure points up to 19.5 kbar. The frequency of the QIOs continuously increases from 210 T at $p = 0.0$ kbar up to 330 T at $p = 19.5$ kbar. As the frequency of QIOs corresponds directly to the k -space area enclosed

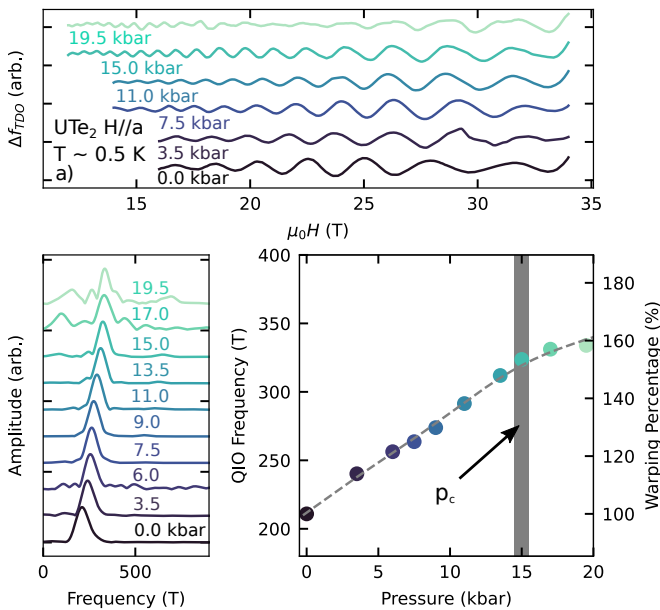


FIG. 2. (a) QIOs in the contactless resistivity of UTe_2 for $H \parallel a$ measured by the change in resonant frequency of a TDO circuit, Δf_{TDO} , at various pressures as indicated. Oscillations have been rescaled to be visible on the same scale. (b) Fast Fourier transforms of the QIOs at each measured pressure point taken over a 16 - 30 T window. (c) QIO frequency plotted versus pressure, showing a smooth increase in frequency with compression. The right hand axis gives the FS warping percentage corresponding to increased QIO frequency.

by the interference paths [34] – similarly to how dHvA and SdH oscillations are related to enclosed orbital areas by the Onsager relation [1, 35] – this indicates that the red shaded area of Fig. 1b has increased in size by a factor of 1.6 from 0 to 19.5 kbar due to the enhanced warping of the FS cylinders with pressure.

In Figure 3 we plot the magnetic field–pressure phase diagram of UTe_2 reported for $H \parallel a$ [20, 21], along with FS simulations showing the cylindrical warping at ambient pressure and at 20 kbar. Ambient-pressure superconductivity with a single-component order parameter [36, 37] has been reported to give way to three additional distinct superconducting phases under pressure for $H \parallel a$ [20, 21]. How these phases may relate to other superconducting states observed for different magnetic field orientations remains the subject of investigation [16, 18, 19, 23–25, 38–41]

We measured QIOs for $H \parallel a$ at 10 incremental pressure points (Fig. 2), at five of which we performed temperature–dependence studies as plotted in Figure 4. For each of these pressures we fit the temperature dependence of the QIO amplitude to the standard Lifshitz-Kosevich formula [1, 4]. This yields an apparent effective mass for the QIOs, which reflects the difference in the effective masses of the two quasiparticle trajectories – one along the electron-type FS sheet and the other along

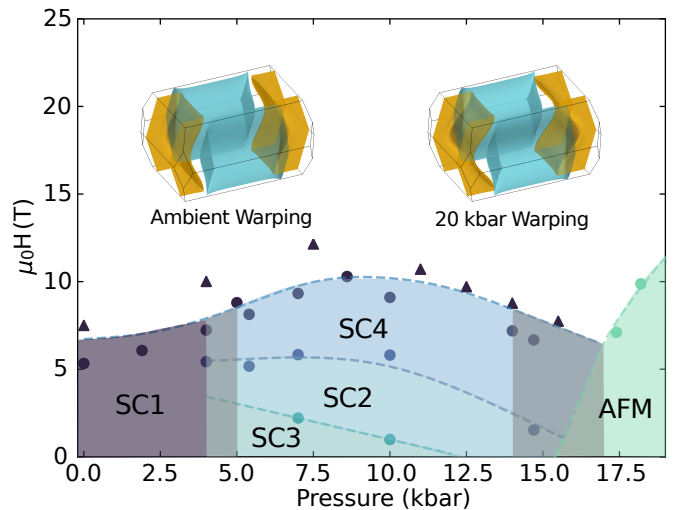


FIG. 3. Superconducting phase diagram of UTe_2 under hydrostatic pressure for applied magnetic field $H \parallel a$. Circular data points are reproduced from refs. [20, 21] whereas triangular points are from this study. Upper insets give simulations of the degree of warping of the cylindrical Fermi sheets at ambient pressure and 19.5 kbar that is indicated by the QIO frequency evolution in Fig. 2.

the hole-type sheet – which combine to give these QIOs (Fig. 1b). The temperature dependence of the QIO amplitude is given by the derivative of the phase ϕ along each interference trajectory with respect to quasiparticle energy E_k [10, 42, 43]. If we express the two trajectories as λ, λ' we may write the apparent effective mass as $m_{\lambda, \lambda'}^* = \frac{e\hbar\mu_0 H}{2\pi} \left| \frac{\partial(\phi_\lambda - \phi_{\lambda'})}{\partial E_k} \right| = |m_\lambda^* - m_{\lambda'}^*|$ where e is the elementary charge and \hbar the reduced Planck constant [13, 34, 42]. It is this peculiar property of QIOs – that their apparent effective mass is given by the *difference* between the conventional QO masses for paths λ, λ' – that enables them to be observed at considerably higher temperatures than dHvA QOs. This is especially true in a heavy fermion system like UTe_2 in which, depending on the magnetic field tilt angle, dHvA experiments have observed effective masses ranging from 32-78 m_e [28, 29]. In contrast, the QIO apparent effective mass for $H \parallel a$ at ambient pressure is considerably lower at only 1.52 m_e . This indicates that the Fermi velocity, $v_F(\mathbf{k})$, is similar over the two arcs that bound the red shaded area in Fig. 1b.

Figure 5 shows the pressure dependence of m^* . We observe a strong initial enhancement of m^* with pressure, starting at 1.52 m_e at ambient pressure and reaching a maximum of 2.43 m_e at 15.0 kbar – 60% higher. For further increasing pressure, m^* drops back slightly, reaching 1.99 m_e at our highest pressure point of 19.5 kbar and showing a clear peak near p_c .

Discussion – The location in k -space of the quasiparticle trajectories responsible for the QIOs probed in this study is very well defined (by the red shaded area in

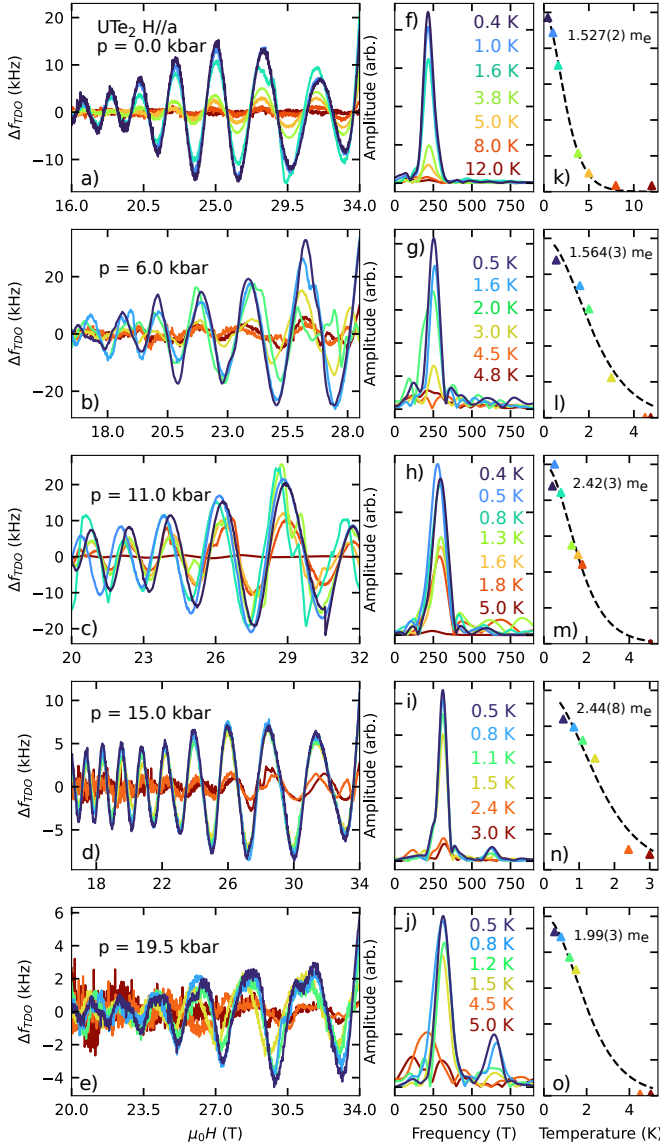


FIG. 4. (a-e) QIOs at incremental pressures as labelled, with corresponding fast Fourier transform (FFT) frequency spectra (f-j) and FFT peak amplitudes plotted versus temperature (k-o). A single oscillation with frequency 200 – 350 T is observed at all pressures, complemented by a second harmonic of increasing amplitude at higher pressures. The colours of the data at each pressure (i.e. of each row of panels) correspond to the temperatures listed by the FFT spectra. Apparent effective masses are extracted from a Lifshitz-Kosevich fit [4] and expressed in terms of the bare electron mass m_e .

Fig. 1b). Therefore, our measurements tell us precisely which sections of the FS sheets undergo a relative change in m^* as a function of pressure.

These findings can be interpreted in terms of a tight binding calculation (see Supplementary Materials for details) based on the model by Ishizuka and Yanase [44] where hopping parameters were modified to fit dHvA measurements [28, 29]. The tight binding model incorporates Te p and U d orbitals that independently produce

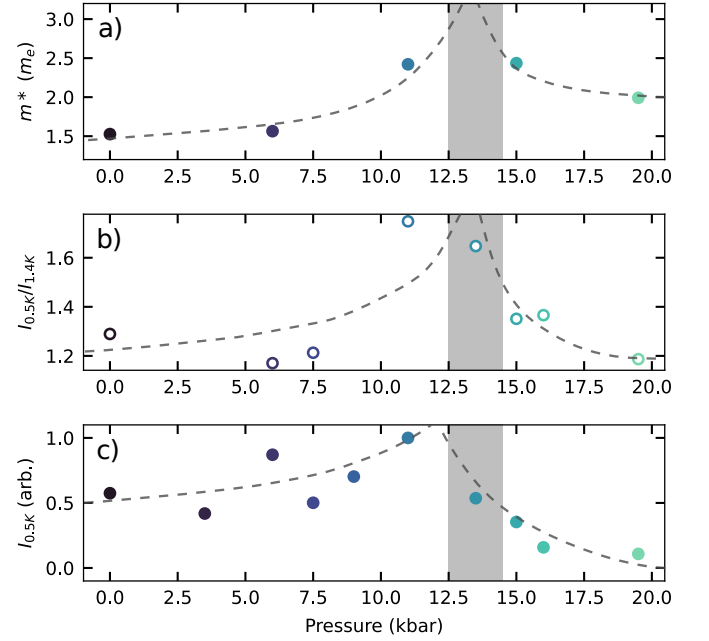


FIG. 5. (a) The pressure dependence of the apparent effective masses of a -axis QIOs in UTe_2 showing an enhancement around the critical pressure of $p_c \approx 15$ kbar. (b) The ratio of the FFT amplitudes of the QIOs at ^3He base temperature (≈ 0.5 K) to that at ^4He base temperature (≈ 1.4 K). This gives a proxy for the mass variation, for a larger number of pressure points compared to panel (a). Amplitudes are rescaled according to the LK curve for an oscillatory component with $m^* = 2m_e$ to account for small temperature discrepancies between pressures (details given in the Supplementary Materials). (c) The amplitude of the QIOs at 0.5 K as a function of pressure, again rescaled according to the LK curve for an oscillation with $m^* = 2m_e$, showing a slight enhancement of QIO amplitude towards p_c , with a subsequent decay beyond p_c .

quasi-1D sheets in the b and a directions, respectively, and hybridise to produce a quasi-2D cylindrical Fermi surface as seen in earlier models [45, 46]. Our calculation supplements these with U f states just above the Fermi energy. Increasing the hybridisation of the f states with the p and d states mixes f -character into the states near the Fermi energy and changes the geometry of the Fermi surface, increasing the degree of warping. Figure 6 illustrates how the f -orbital contribution at the Fermi level varies as a function of \mathbf{k} . Blue regions have low f -contribution, whereas red areas possess strong f -type character.

To capture how the degree of f -orbital contribution relates to the warping of the cylindrical FS sheets, we calculated the z -component of the normal vector to the FS sheets as a function of the f -weighting (Fig. 6e). We find somewhat surprisingly that for zero f -weighting there is zero projection normal to k_z , and therefore that the FS would be properly 2D in such a scenario. By contrast, as the f -weighting is increased, so too is the normal projection to k_z . The experimental finding that the warping

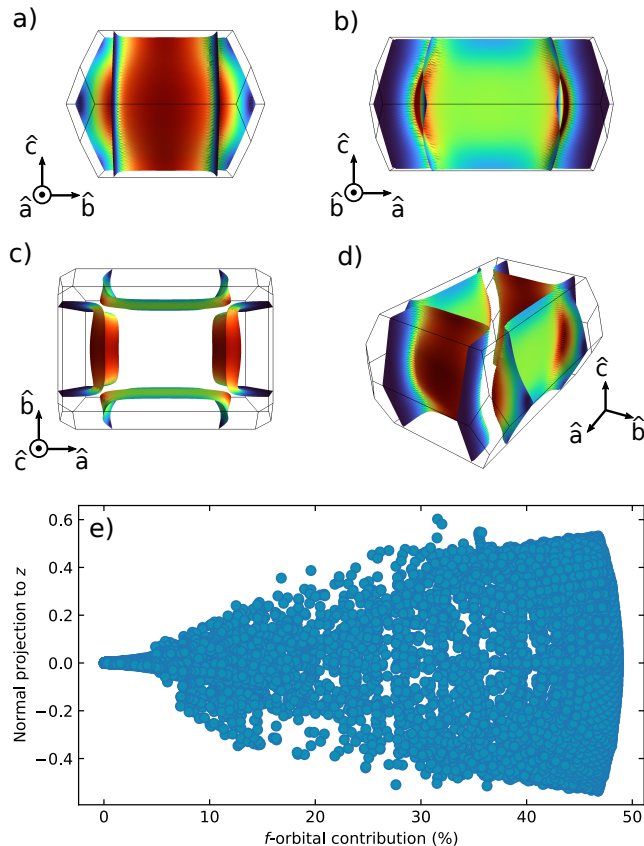


FIG. 6. (a-d) The ambient pressure FS of UTe_2 , constructed from our tight binding approximation guided by dHvA measurements [28, 29] (calculational details given in the Supplementary Materials). Red (blue) colouring denotes areas of high (low) f -orbital contribution. Areas of higher curvature are found where there is a high f -contribution at the Fermi level. (e) Using the z -component of the normal to the Fermi surface as a measure of how 3D-like the cylindrical FS warping is, we see that for no f -orbital contribution there is no z -component to the FS normal. Therefore, in the absence of f electrons the calculated FS is strictly 2D. Conversely, increasing f -electron contribution is associated with an increase in the 3D character of the FS cylinders, caused by an increase in the cylindrical warping.

of the UTe_2 FS cylinders smoothly increases under pressure (Fig. 2) is within this model succinctly explained by a continuous increase in f -orbital character at the Fermi level.

Further information can be obtained from the second harmonic in the QIO spectra (Fig. 4), which grows with pressure and is especially pronounced at 15.0 kbar at 19.5 kbar. The second harmonic relates to quasiparticles performing two laps of the red shaded area in Fig 1b – i.e. starting at the top of the first Brillouin zone, with one tunnelling across and not recombining again until the bottom of the second Brillouin zone. As the probability for magnetic breakdown to occur has the field dependency of $P = \exp(-B_0/B)$ for breakdown field B_0 [1, 7],

this increase in the ratio of the second harmonic amplitude to that of the first is characteristic of the FS sheets getting closer together in reciprocal space. This raises the possibility of a Lifshitz transition at higher pressures beyond 19.5 kbar.

Prior experimental studies of UTe_2 have tracked the evolution under pressure of A , the quadratic temperature coefficient of the resistivity given by $\rho = \rho_0 + AT^2$ [47, 48]. A clear peak in A was observed in proximity to p_c . As $A^{0.5} \propto m^*$ (where here m^* is strictly the effective carrier mass [49], not the apparent QIO mass), this finding was proposed to indicate the presence of an AFM quantum critical point at p_c [47]. Our observation of a peak in m^* around p_c provides microscopic evidence in favour of this scenario. In contrast to the peak in the effective mass near p_c , the onset of AFM order is not reflected in the QIO frequency, which continues to grow smoothly with increased pressure up to the maximum pressure of 19.5 kbar reached in this study, albeit more gradually above p_c . This indicates that, at least in the high-field paramagnetic normal state in which the QIOs are observed, the FS deforms continuously, with no indication of a sudden reconstruction. Inside the AFM state the FS may be markedly different, but no oscillatory features could be resolved in the contactless conductivity below the moderately low fields ($\mu_0 H \lesssim 10$ T) at which the AFM state is suppressed for $H \parallel a$ at $T = 0.4$ K. The peak of m^* in this high field paramagnetic phase indicates that quantum critical behaviour may be expected at lower fields.

It has previously been conjectured [24] that, for $p > p_c$, the field polarised paramagnetic state, which is found at ambient pressures for $\mu_0 H_b \gtrsim 34$ T and comes down to lower fields at higher pressures [16, 39, 50], is also accessed for $H \parallel a$. However, we observed no signatures in our TDO measurements that would signal the metamagnetic transition to the field polarised phase. Instead, it appears that the field polarised state is not accessible for $H \parallel a$, at least not for $p \leq 19.5$ kbar with $H \leq 41.5$ T and $T \geq 0.4$ K. The proposal [41] that above p_c the f -electrons are largely localized in UTe_2 appears to be inconsistent with our findings, at least for $\mu_0 H \gtrsim 10$ T, as our data suggest continuously increasing f -orbital character under increasing compression. This raises the question of how the dual nature of localization and itinerancy of $5f$ electrons [51, 52] might evolve in UTe_2 at $p > p_c$ from $0 \leq \mu_0 H \lesssim 10$ T – and thus of what role the incommensurate AFM order and its associated magnetic fluctuations may play in forming the numerous exotic superconductive phases spanning the pressure phase landscape [19, 20, 39, 40, 47].

In summary, we tracked key features of the Fermi surface of UTe_2 with applied pressure up to 19.5 kbar by measuring quantum interference oscillations (QIOs) using a contactless conductivity technique. We observe a smooth increase in QIO frequency with pressure for magnetic field oriented along the crystallographic a -axis. This indicates that the ambient pressure Fermi surface

deforms continuously with pressure across the critical pressure, with no evidence of a Fermi surface reconstruction in the high magnetic field paramagnetic state. We show that this deformation is consistent with increasing f -orbital contribution at the Fermi level with increasing pressure. We observe a peak in the apparent effective masses of the QIOs around the critical pressure, providing the first microscopic evidence for the presence of quantum criticality underpinning magnetic phase formation in the high pressure UTe_2 phase landscape.

ACKNOWLEDGMENTS

We are grateful to D.V. Chichinadze, D. Shaffer, J. Schmalian, T. Hazra, A. McCollam, N.R. Cooper, P. Coleman, A.F. Bangura and especially A. Carrington for stimulating discussions. We thank T.J. Brumm for technical assistance. This project was supported by the EPSRC of the UK (grants EP/X011992/1 & EP/R513180/1). A portion of this work was performed at the National High Magnetic Field Laboratory, which is supported by National Science Foundation Cooper-

ative Agreement No. DMR-2128556 and the State of Florida. Crystal growth and characterization were performed in MGML (mgml.eu), which is supported within the program of Czech Research Infrastructures (project no. LM2023065). We acknowledge financial support by the Czech Science Foundation (GACR), project No. 22-22322S. A portion of this work was carried out at the Synergetic Extreme Condition User Facility (SECUF). T.I.W. and A.G.E. acknowledge support from QuantEmX grants from ICAM and the Gordon and Betty Moore Foundation through Grants GBMF5305 & GBMF9616. Computational simulations were performed using the the ARCHER2 UK National Supercomputing Service (<https://www.archer2.ac.uk>). A.G.E. acknowledges support from the Henry Royce Institute for Advanced Materials through the Equipment Access Scheme enabling access to the Advanced Materials Characterisation Suite at Cambridge, grants EP/P024947/1, EP/M000524/1 & EP/R00661X/1; and from Sidney Sussex College (University of Cambridge).

-
- [1] D. Shoenberg, *Magnetic Oscillations in Metals* (Cambridge University Press, Cambridge, UK, 1984).
- [2] L. Schubnikow and W. J. de Haas, New phenomena in the change in resistance of bismuth crystals in a magnetic field at the temperature of liquid hydrogen (I), *Proc. Netherlands Roy. Acad. Sci.* **130**, 363 (1930).
- [3] W. J. de Haas and P. M. van Alphen, The dependence of the susceptibility of diamagnetic metals upon the field, *Proc. Netherlands Roy. Acad. Sci.* **130**, 1106 (1930).
- [4] I. M. Lifshitz and A. M. Kosevich, *Sov. Phys. JETP* **2**, 636 (1956).
- [5] M. H. Cohen and L. M. Falicov, Magnetic Breakdown in Crystals, *Phys. Rev. Lett.* **7**, 231 (1961).
- [6] A. B. Pippard, Quantization of coupled orbits in metals, *Proc. Roy. Soc. A* **270**, 1 (1962).
- [7] R. G. Chambers, Magnetic breakdown in real metals, *Proc. Phys. Soc.* **88**, 701 (1966).
- [8] H. Shiba and H. Fukuyama, A Quantum Theory of Galvanomagnetic Effect in Metals with Magnetic Breakdown. I, *J. Phys. Soc. Jpn.* **26**, 910 (1969).
- [9] R. Stark and C. Friedberg, Quantum interference of electron waves in a normal metal, *Phys. Rev. Lett.* **26**, 556 (1971).
- [10] N. Harrison, J. Caulfield, J. Singleton, P. Reinders, F. Herlach, W. Hayes, M. Kurmoo, and P. Day, Magnetic breakdown and quantum interference in the quasi-two-dimensional superconductor κ -(BEDT-TTF) $_2$ Cu(NCS) $_2$ in high magnetic fields, *J. Phys.: Condens. Matter* **8**, 5415 (1996).
- [11] J. Singleton, Studies of quasi-two-dimensional organic conductors based on BEDT-TTF using high magnetic fields, *Rep. Prog. Phys.* **63**, 1111 (2000).
- [12] C. Broyles, Z. Rehfuss, H. Siddiquee, J. A. Zhu, K. Zheng, M. Nikolo, D. Graf, J. Singleton, and S. Ran, Revealing a 3D Fermi Surface Pocket and Electron-Hole Tunneling in UTe_2 with Quantum Oscillations, *Phys. Rev. Lett.* **131**, 036501 (2023).
- [13] T. I. Weinberger, Z. Wu, D. E. Graf, Y. Skourski, A. Cabala, J. Pospisil, J. Prokleska, T. Haidamak, G. Bastien, V. Sechovsky, G. G. Lonzarich, M. Valiska, F. M. Grosche, and A. G. Eaton, Quantum interference between quasi-2D Fermi surface sheets in UTe_2 (2023), [arXiv:2307.00568](https://arxiv.org/abs/2307.00568) [cond-mat.supr-con].
- [14] K. Stöwe, Contributions to the crystal chemistry of uranium tellurides: III. Temperature-dependent structural investigations on uranium ditelluride, *J. Solid State Chem.* **127**, 202 (1996).
- [15] S. Ran, C. Eckberg, Q. P. Ding, Y. Furukawa, T. Metz, S. R. Saha, I. L. Liu, M. Zic, H. Kim, J. Paglione, and N. P. Butch, Nearly ferromagnetic spin-triplet superconductivity, *Science* **365**, 684 (2019).
- [16] D. Aoki, J. P. Brison, J. Flouquet, K. Ishida, G. Knebel, Y. Tokunaga, and Y. Yanase, Unconventional superconductivity in UTe_2 , *J. Phys. Condens. Matter* **34**, 243002 (2022).
- [17] H. Sakai, P. Opletal, Y. Tokiwa, E. Yamamoto, Y. Tokunaga, S. Kambe, and Y. Haga, Single crystal growth of superconducting UTe_2 by molten salt flux method, *Phys. Rev. Materials* **6**, 073401 (2022).
- [18] S. Ran, I. L. Liu, Y. S. Eo, D. J. Campbell, P. M. Neves, W. T. Fuhrman, S. R. Saha, C. Eckberg, H. Kim, D. Graf, F. Balakirev, J. Singleton, J. Paglione, and N. P. Butch, Extreme magnetic field-boosted superconductivity, *Nat. Phys.* **15**, 1250 (2019).
- [19] D. Braithwaite, M. Vališka, G. Knebel, G. Lapertot, J. P. Brison, A. Pourret, M. E. Zhitomirsky, J. Flouquet, F. Honda, and D. Aoki, Multiple superconducting phases in a nearly ferromagnetic system, *Communications Physics* **2**:1 **2**, 1 (2019).
- [20] D. Aoki, F. Honda, G. Knebel, D. Braithwaite, A. Nakamura, D. Li, Y. Homma, Y. Shimizu, Y. J. Sato, J.-P. Brison, *et al.*, Multiple superconducting phases and unusual enhancement of the upper critical field in UTe_2 , *J. Phys. Soc. Jpn.* **89**, 053705 (2020).

- [21] G. Knebel, M. Kimata, M. Vališka, F. Honda, D. Li, D. Braithwaite, G. Lapertot, W. Knafo, A. Pourret, Y. J. Sato, *et al.*, Anisotropy of the upper critical field in the heavy-fermion superconductor UTe_2 under pressure, *J. Phys. Soc. Jpn.* **89**, 053707 (2020).
- [22] D. Aoki, M. Kimata, Y. J. Sato, G. Knebel, F. Honda, A. Nakamura, D. Li, Y. Homma, Y. Shimizu, W. Knafo, *et al.*, Field-induced superconductivity near the superconducting critical pressure in UTe_2 , *J. Phys. Soc. Jpn.* **90**, 074705 (2021).
- [23] Z. Wu, T. I. Weinberger, J. Chen, A. Cabala, D. V. Chichinadze, D. Shaffer, J. Pospisil, J. Prokleska, T. Haidamak, G. Bastien, V. Sechovsky, A. J. Hickey, M. J. Mancera-Ugarte, S. Benjamin, D. E. Graf, Y. Skourski, G. G. Lonzarich, M. Vališka, F. M. Grosche, and A. G. Eaton, Enhanced triplet superconductivity in next generation ultraclean UTe_2 (2023), [arXiv:2305.19033](https://arxiv.org/abs/2305.19033).
- [24] S. K. Lewin, C. E. Frank, S. Ran, J. Paglione, and N. P. Butch, A Review of UTe_2 at High Magnetic Fields, *Rep. Prog. Phys.* (2023).
- [25] T. Helm, M. Kimata, K. Sudo, A. Miyata, J. Stirnat, T. Förster, J. Hornung, M. König, I. Sheikin, A. Pourret, *et al.*, Field-induced compensation of magnetic exchange as the possible origin of reentrant superconductivity in UTe_2 , *Nat. Commun.* **15**, 37 (2024).
- [26] W. Knafo, T. Thebault, P. Manuel, D. D. Khalyavin, F. Orlandi, E. Ressouche, K. Beauvois, G. Lapertot, K. Kaneko, D. Aoki, D. Braithwaite, G. Knebel, and S. Raymond, Incommensurate antiferromagnetism in UTe_2 under pressure (2023), [arXiv:2311.05455](https://arxiv.org/abs/2311.05455) [cond-mat.str-el].
- [27] L. Miao, S. Liu, Y. Xu, E. C. Kotta, C.-J. Kang, S. Ran, J. Paglione, G. Kotliar, N. P. Butch, J. D. Denlinger, and L. A. Wray, Low Energy Band Structure and Symmetries of UTe_2 from Angle-Resolved Photoemission Spectroscopy, *Phys. Rev. Lett.* **124**, 076401 (2020).
- [28] D. Aoki, H. Sakai, P. Opletal, Y. Tokiwa, J. Ishizuka, Y. Yanase, H. Harima, A. Nakamura, D. Li, Y. Homma, Y. Shimizu, G. Knebel, J. Flouquet, and Y. Haga, First Observation of the de Haas-van Alphen Effect and Fermi Surfaces in the Unconventional Superconductor UTe_2 , *J. Phys. Soc. Jpn.* **91**, 083704 (2022).
- [29] A. G. Eaton, T. I. Weinberger, N. J. M. Popiel, Z. Wu, A. J. Hickey, A. Cabala, J. Pospíšil, J. Prokleska, T. Haidamak, G. Bastien, P. Opletal, H. Sakai, Y. Haga, R. Nowell, S. M. Benjamin, V. Sechovský, G. G. Lonzarich, F. M. Grosche, and M. Vališka, Quasi-2D Fermi surface in the anomalous superconductor UTe_2 , *Nat. Commun.* **15**, 223 (2024).
- [30] S. Klotz, J. Chervin, P. Munsch, and G. Le Marchand, Hydrostatic limits of 11 pressure transmitting media, *J. Phys. D: Appl. Phys.* **42**, 075413 (2009).
- [31] G. J. Piermarini, S. Block, J. D. Barnett, and R. A. Forman, Calibration of the pressure dependence of the R1 ruby fluorescence line to 195 kbar, *J. Appl. Phys.* **46**, 2774 (1975).
- [32] C. T. Van Degrift, Tunnel diode oscillator for 0.001 ppm measurements at low temperatures, *Rev. Sci. Instr.* **46**, 599 (2008).
- [33] K. Semeniuk, H. Chang, J. Baglo, S. Friedemann, S. W. Tozer, W. A. Coniglio, M. B. Gamza, P. Reiss, P. Alireza, I. Leermakers, *et al.*, Truncated mass divergence in a Mott metal, *Proc. Natl. Acad. Sci. USA* **120**, e2301456120 (2023).
- [34] M.I. Kaganov and A.A. Slutskin, Coherent magnetic breakdown, *Phys. Rep.* **98**, 189 (1983).
- [35] L. Onsager, Interpretation of the de Haas-van Alphen effect, *Philos. Mag.* **43**, 1006 (1952).
- [36] F. Theuss, A. Shragai, G. Grissonnanche, I. M. Hayes, S. R. Saha, Y. S. Eo, A. Suarez, T. Shishidou, N. P. Butch, J. Paglione, and B. J. Ramshaw, Single-Component Superconductivity in UTe_2 at Ambient Pressure (2023), [arXiv:2307.10938](https://arxiv.org/abs/2307.10938).
- [37] P. F. S. Rosa, A. Weiland, S. S. Fender, B. L. Scott, F. Ronning, J. D. Thompson, E. D. Bauer, and S. M. Thomas, Single thermodynamic transition at 2 K in superconducting UTe_2 single crystals, *Commun. Mater.* **3**, 33 (2022).
- [38] W. Knafo, M. Nardone, M. Vališka, A. Zitouni, G. Lapertot, D. Aoki, G. Knebel, and D. Braithwaite, Comparison of two superconducting phases induced by a magnetic field in UTe_2 , *Commun. Phys.* **4**, 40 (2021).
- [39] W.-C. Lin, D. J. Campbell, S. Ran, I.-L. Liu, H. Kim, A. H. Nevidomskyy, D. Graf, N. P. Butch, and J. Paglione, Tuning magnetic confinement of spin-triplet superconductivity, *npj Quantum Mater.* **5**, 68 (2020).
- [40] S. Ran, S. R. Saha, I.-L. Liu, D. Graf, J. Paglione, and N. P. Butch, Expansion of the high field-boosted superconductivity in UTe_2 under pressure, *npj Quantum Mater.* **6**, 75 (2021).
- [41] K. Kinjo, H. Fujibayashi, H. Matsumura, F. Hori, S. Kitagawa, K. Ishida, Y. Tokunaga, H. Sakai, S. Kambe, A. Nakamura, Y. Shimizu, Y. Homma, D. Li, F. Honda, and D. Aoki, Superconducting spin reorientation in spin-triplet multiple superconducting phases of UTe_2 , *Sci. Adv.* **9**, eadg2736 (2023).
- [42] M. V. Kartsovnik, G. Y. Logvenov, T. Ishiguro, W. Biberacher, H. Anzai, and N. D. Kushch, Direct Observation of the Magnetic-Breakdown Induced Quantum Interference in the Quasi-Two-Dimensional Organic Metal κ -(BEDT-TTF) $_2\text{CU}(\text{NCS})_2$, *Phys. Rev. Lett.* **77**, 2530 (1996).
- [43] N. Harrison, R. G. Goodrich, J. J. Vuillemin, Z. Fisk, and D. G. Rickel, Quantum Interference in LaB_6 , *Phys. Rev. Lett.* **80**, 4498 (1998).
- [44] J. Ishizuka and Y. Yanase, Periodic Anderson model for magnetism and superconductivity in UTe_2 , *Phys. Rev. B* **103**, 094504 (2021).
- [45] A. H. Nevidomskyy, Stability of a Nonunitary Triplet Pairing on the Border of Magnetism in UTe_2 (2020), [2001.02699](https://arxiv.org/abs/2001.02699).
- [46] D. Shaffer and D. V. Chichinadze, Chiral superconductivity in UTe_2 via emergent C_4 symmetry and spin-orbit coupling, *Phys. Rev. B* **106**, 014502 (2022).
- [47] S. M. Thomas, F. B. Santos, M. H. Christensen, T. Asaba, F. Ronning, J. D. Thompson, E. D. Bauer, R. M. Fernandes, G. Fabbris, and P. F. Rosa, Evidence for a pressure-induced antiferromagnetic quantum critical point in intermediate-valence UTe_2 , *Sci. Adv.* **6**, 8709 (2020).
- [48] M. Vališka, W. Knafo, G. Knebel, G. Lapertot, D. Aoki, and D. Braithwaite, Magnetic reshuffling and feedback on superconductivity in UTe_2 under pressure, *Physical Review B* **104**, 214507 (2021).
- [49] P. Coleman, *Introduction to Many-Body Physics* (Cambridge University Press, Cambridge, UK, 2015).
- [50] A. Miyake, Y. Shimizu, Y. J. Sato, D. Li, A. Nakamura, Y. Homma, F. Honda, J. Flouquet, M. Tokunaga, and

- D. Aoki, Metamagnetic Transition in Heavy Fermion Superconductor UTe₂, *J. Phys. Soc. Jpn.* **88** (2019).
- [51] G. Zwicknagl and P. Fulde, The dual nature of $5f$ electrons and the origin of heavy fermions in U compounds, *J. Phys.: Condens. Matter* **15**, S1911 (2003).
- [52] A. Amorese, M. Sundermann, B. Leedahl, A. Marino, D. Takegami, H. Gretarsson, A. Gloskovskii, C. Schlueter, M. W. Haverkort, Y. Huang, *et al.*, From antiferromagnetic and hidden order to Pauli paramagnetism in UM_2Si_2 compounds with $5f$ electron duality, *Proc. Natl. Acad. Sci. USA* **117**, 30220 (2020).